Nonconventional Angle-Of-Attack Control Strategy for Reducing the Airspeed During the Fixed-Wing Drone Landing

Armando Alatorre, Pedro Castillo Garcia, Rogelio Lozano

Nonconventional angle-of-attack control strategy for reducing the airspeed during the fixed-wing drone landing

A. Alatorre[1,2], P. Castillo[1] and R. Lozano[1,2].

***Abstract*— In this work, a control strategy for landing, with minimum airspeed, a fixed-wing drone with classical configuration on a touchdown point is presented. In this crucial and critic landing phase of this kind of aircrafts the challenge is to absorb the drone's airspeed without loss its controllability. Our strategy proposes a scientific solution for a safe landing by controlling the angle of attack of the drone assuring its stability during all this stage. In our analysis, a flight scheme composed by a cruise flight and a landing scheme is considered. The control strategy obtained from the Lyapunov theory proposes a critic descending angle to obtain a maximum airspeed reduction. In addition, an observer is proposed for estimating external aerodynamics parameters and compensate them in closed-loop system. Numerical validation corroborates the well performance of the proposed control algorithms.**

I. Introduction

Unmanned aerial vehicles (UAVs) have presented great potential for a wide range of applications in the military and civil fields. In military missions, they have been used to monitor risk areas [1], convoy protection [2], target reconnaissance [3], and tracking of ground vehicles [4]. Some civil applications are the searching operations of marine resources [5], agriculture activities [6], detection of forest fires [7], and search-rescue missions [8]. Additionally, UAVs have been applied to the delivery of critical medical supplies and blood packs, which allows the reduction of distribution time [9].

UAVs are commonly classified as multi-rotor and fixed-wing vehicles. A multi-rotor vehicle is comprised of more than two rotors. This configuration presents a vertical thrust, allowing hover flights, high-precision maneuvers, take-off, and land vertically [10]. Nevertheless, its flight durability due to the energy consumption of the rotors is their main drawback. Otherwise, fixed-wing vehicles have more durability since the lift force generated by its wings allows the low energy consumption of its motor [12]. Fixed-wing vehicles are used for missions of long distances, high altitudes, and speeds [11]. One limitation of the fixed-wing vehicles is the necessity of a long flat runway for landing. In fact, the landing maneuver is considered a dangerous flight stage, since the aircraft must reduce its kinetic energy before landing, and can be affected by wind disturbances producing instability and crashing the vehicle. Therefore, landing this kind of aircrafts in reduced areas increases the challenge to avoid accidents and damage to their structures.

[1]Université de technologie de Compiègne, CNRS, Heudiasyc (Heuristics and Diagnosis of Complex Systems), CS 60319 - 60203 Compiègne Cedex, France. (aalatorr, castillo, rlozano)@hds.utc.fr

[2]Center of Research and Advanced Studies of the National Polytechnic Institute (CINVESTAV), Mexico.

The scientific community has proposed solutions based on control theory for a safe autonomous landing of a fixed-wing drone on a runway such as in [13]. The authors divide a landing regime into descending flight, flare maneuver, and taxiing. The aircraft requires high precision for an automatic landing, thus some aircraft's controls are supported by computer vision algorithms to align the vehicle with the runway or to estimate the position and speed of the aircraft with respect to a target such as in [14] and [15].

In the literature, solutions addressing the research on landing problems in reduced zones can be found. These solutions are focused on recovery systems. Some of them consist of directing the aircraft towards an inflatable or nets, implying the drastic reduction of its kinetic energy such as in [16] and [17]. Other capture techniques use tensed or elastic cables to brake the drone such as in [18]. Thus, some capture maneuvers are considered aggressive increasing the possibility of damage the vehicle since most of the recovery systems do not reduce the kinetic energy of the aircraft.

Focusing on the airspeed reduction maneuver, a popular aerial maneuver performed by aerobatic airplanes can be found. This maneuver is the Pugachev's cobra which reduces its airspeed during the flight by increasing the angle of attack (AOA) of the aircraft, reaching higher angles than ninety degrees. In this maneuver the drag force is highly increased allowing the absorption of the kinetic energy [19]. After that, the aircraft recovers its flight thanks to its aerodynamic capabilities to generate lift force to high angles of attack. Nevertheless, Pugachev's cobra maneuver is impossible to be performed by a classical aircraft, since, if the drone reaches angles beyond the stall angle, its lift force tends to be drastically reduced and the drag force increases. The stall effect can be produced the loss of aircraft's controllability.

Some solutions are proposed, in the literature, for reaching regions close to the stall angles. For example, in [20], the authors propose an emergency strategy for a fixed-wing vehicle to avoid a collision with another one in the landing stage. The aircraft reduces its airspeed, increasing the AOA to deep stall conditions. In [21], the authors propose a model reference control to stabilize the altitude and airspeed where the deep stall conditions are reached by the regulation of airspeed. Another alternative solution is the modification of the airplane's structure which has been studied to obtain aerodynamic features such as in [22]. In this work, the authors include four thrusters in a fixed-wing vehicle, and propose a deep stall maneuver to reduce the airspeed. After that, the thrusters are controlled to perform

a vertical landing. Similarly, a landing scheme is proposed for a variable forward-swept aircraft in [23]. The strategy focuses on controlling the AOA, and its stability analysis is based on Lyapunov theory. However, the airspeed effects are neglected by the aerodynamic coefficients, thus, the stability is not guaranteed in the transition from a cruise flight to a descending flight. Moreover, in [24], the authors proposed a control strategy for an automatic landing based on deep stall conditions at a fixed coordinate. The strategy is based on a Model Predictive Control (MPC). The above strategy was improved with the stabilization of the lateral dynamics in [25], and then, a Dubins path stage is added before starting the descending flight in [26]. However, the deep stall conditions can be a problem for a fixed-wing drone affected by external disturbances since the aircraft can be easily out of the deep stall region. Thus, the flight recuperation of the aircraft would be impossible by the loss of lift force.

In this work, we propose a control strategy for landing a fixed-wing vehicle on a desired coordinate. The airspeed reduction is reached carrying the aircraft close to its limit angle of attack (stall angle). For analyzing the descending flight, a cruise flight with constant altitude and speed is considered. The descending angle is studied to obtain a maximum airspeed reduction, avoiding the loss of controllability of the aerial system. Moreover, a reference function is proposed to reach the maximum pitch angle which implies that the AOA increases until the stall angle. The proposed control strategy considers the two control inputs available in it. The first one, the engine control input, is used to guide the aircraft, while the second one, the elevator deflection, will control the pitch angle. The control loop system is computed using estimated aerodynamics and external disturbances obtained from an observer algorithm. The control algorithms are developed using the Lyapunov theory. The whole strategy is validated in simulations showing the well performance of the system.

The manuscript is organized as follows: the problem statement and preliminaries are given in Section II. The landing control strategy composed of the guidance and pitch algorithms is developed in Section III. Main graphs from simulation results when validating the proposed strategy are shown in Section IV. Finally, concluding remarks and future research directions are presented in Section V.

II. Preliminaries and problem statement

The landing maneuver for a commercial airplane consists of a controlled and restricted airspeed reduction by increasing slowly the angle of attack. This maneuver assures all the time the stability balance of the lift force and by consequence of the aerial system. Once the airplane reaches the touchdown point of the runway, the kinetic energy of the aircraft can be absorbed using their spoilers.

This kind of methodologies for landing an airplane is not useful for doing it in reduced spaces. Therefore, there is a great scientific challenge here that it is not yet solved. We propose a solution based on the control theory and considering a high and critic angle of attack for reducing the airspeed when the airplane is landing in such away that it can be landed on a desired coordinate. The scientific challenge here will be to assure the stability of the system when it reaches a critic angle of attack that could be it unstable. It is considered a complex flight maneuver due to the high angles of attack close to the stall angle α_{stall}.

The strategy will be mainly obtained for the landing stage considering that the lateral and yaw dynamics are already stabilized. Therefore, the analysis will be done for the longitudinal dynamics.

A. Longitudinal motion equation for a fixed-wing drone

The nonlinear equations for the longitudinal dynamics for a fixed-wing drone can be written as [27]:

$$\dot{x} = u\cos\theta + w\sin\theta, \quad (1)$$

$$\dot{z} = u\sin\theta - w\cos\theta, \quad (2)$$

$$\dot{u} = -qw - g\sin\theta + \frac{\rho V_a^2 S}{2m}A_u + \frac{\rho S_h C_h}{2m}P_u + d_u, \quad (3)$$

$$\dot{w} = qu + g\cos\theta + \frac{\rho V_a^2 S}{2m}A_w + d_w, \quad (4)$$

$$\dot{\theta} = q, \quad (5)$$

$$\dot{q} = \frac{\rho V_a^2 Sc}{2J_y}\left[C_m(\alpha) + Cm_q\frac{cq}{2V_a} + Cm_{\delta e}\,\delta_e\right] + d_q. \quad (6)$$

where (x, z) represent the vehicle position in the inertial frame. The linear velocities (u, w) and the pitch angular velocity $q = \dot{\theta}$ are defined in the vehicle body frame. The gravity force g, the propulsion force P_u, and the aerodynamic forces (A_u, A_w), and moments are involved in the accelerations defined in the body frame. Moreover, external disturbances (d_u, d_w, d_q) are included in its respective dynamic. The control inputs are given by the elevator deflection δ_e and the engine δ_t. The air density is denoted by ρ, and the airspeed by V_a. The vehicle's mass is represented by m and the axis-y inertial element is given as J_y. S defines the surface area of the aircraft wing and c depicts the mean chord of the wing. Finally, the area and the aerodynamic coefficient of the propeller are defined as S_h and C_h, respectively. In addition, A_u and A_w, are composed by elements of the aerodynamic force while P_u includes the propulsion force. They can be represented as

$$A_u = \left[C_X(\alpha) + C_{Xq}(\alpha)\frac{cq}{2V_a} + C_{X\delta_e}(\alpha)\,\delta_e\right], \quad (7)$$

$$P_u = \left[(k_r\delta_t)^2 - V_a^2\right], \quad (8)$$

$$A_w = \left[C_Z(\alpha) + C_{Zq}(\alpha)\frac{cq}{2V_a} + C_{Z\delta e}(\alpha)\delta_e\right], \quad (9)$$

where k_r denotes the engine efficiency constant, and the aerodynamics coefficients are expressed as:

$$C_X(\alpha) = -C_D(\alpha)\cos\alpha + C_L(\alpha)\sin\alpha \quad (10)$$

$$C_{Xq}(\alpha) = -C_{Dq}\cos\alpha + C_{Lq}\sin\alpha \quad (11)$$

$$C_{X\delta e}(\alpha) = -C_{D\delta e}\cos\alpha + C_{L\delta e}\sin\alpha \quad (12)$$

$$C_Z(\alpha) = -C_D(\alpha)\sin\alpha - C_L(\alpha)\cos\alpha \quad (13)$$

$$C_{Z_q}(\alpha) = -C_{Dq}\sin\alpha - C_{Lq}\cos\alpha \quad (14)$$

$$C_{Z\delta_e}(\alpha) = -C_{D\delta e}\sin\alpha - C_{L\delta e}\cos\alpha. \quad (15)$$

$C_{Lq}, C_{L\delta e}, C_{Dq}, C_{D\delta e}$ represent aerodynamic coefficients and can be considered with a constant value. The lift coefficient can be described as

$$C_L(\alpha) = (1-\sigma(\alpha))\left[C_{L_0} + C_{L_\alpha}\alpha\right] + \sigma(\alpha)\left[2\,\mathrm{sgn}(\alpha)\sin^2\alpha\cos\alpha\right], \quad (16)$$

where C_{L_0} represents the lift coefficient when the parameters $\alpha = q = \delta_e = 0$, and $C_{L_\alpha} = \frac{\partial C_L}{\partial \alpha}$. In addition, the function $\sigma(\alpha)$ is given by

$$\sigma(\alpha) = \frac{1 + e^{-M(\alpha-\alpha_0)} + e^{M(\alpha+\alpha_0)}}{\left(1+e^{-M(\alpha-\alpha_0)}\right)\left(1+e^{M(\alpha+\alpha_0)}\right)}, \quad (17)$$

with M and α_0 are positive constants. The sigmoid function describes a piecewise function with a cutoff of α_0 and transition rate M. Similarly, the C_D drag coefficient is defined as

$$C_D(\alpha) = C_{D_p} + 2\ \mathrm{sgn}(\alpha)\sin^3\alpha. \quad (18)$$

where C_{D_p} denotes the parasite drag coefficient. Then, the pitch moment coefficient is expressed as in [28]:

$$C_m(\alpha) = (1-\sigma(\alpha))\left[C_{m_0} + C_{m_\alpha}\alpha\right] + \sigma(\alpha)\left[-1/2\,\mathrm{sgn}(\alpha)\sin^2\alpha\right]. \quad (19)$$

The pitch moment, the lift and drag forces include the behavior for lower and higher angles than the stall angle, [29]. Finally, the airspeed and angle of attack are defined as

$$V_a = \sqrt{u^2+w^2}, \quad (20)$$

$$\alpha = \tan^{-1}\left(\frac{w}{u}\right). \quad (21)$$

B. Airspeed analysis

The airspeed analysis focuses on calculating the minimum velocity of a fixed-wing vehicle to maintain the flight. The airspeed can be considered as function of the angle of attack, i.e., if the AOA is small then, the aircraft navigates to high airspeed, thus, a high AOA represents low velocity. For simplifying this analysis, the external disturbances are not considered. Differentiating (20), it yields

$$\dot{V}_a = \frac{u\dot{u} + w\dot{w}}{V_a}, \quad (22)$$

considering the rotation from the wind to body frames [27], the following expressions can be obtained

$$u = V_a\cos\alpha \quad (23)$$

$$w = V_a\sin\alpha \quad (24)$$

then, (22) can be rewritten as

$$\dot{V}_a = \dot{u}\cos\alpha + \dot{w}\sin\alpha. \quad (25)$$

Proposing $\Delta_\alpha = \frac{w}{u}$ and differentiating (21), it follows

$$\dot{\alpha} = \frac{\dot{\Delta}_\alpha}{1+\Delta_\alpha^2} = \frac{u\dot{w} - w\dot{u}}{u^2+w^2} = \frac{u\dot{w} - w\dot{u}}{V_a^2}. \quad (26)$$

Using (23) and (24), (26) can be rewritten as

$$\dot{\alpha} = \frac{\dot{w}\cos\alpha - \dot{u}\sin\alpha}{V_a}. \quad (27)$$

Therefore,

$$\dot{u} = \frac{\dot{w}\cos\alpha - \dot{\alpha}V_a}{\sin\alpha}. \quad (28)$$

Introducing (28) into (25), it follows

$$\dot{V}_a = \frac{\dot{w}}{\sin\alpha} - \frac{\dot{\alpha}V_a\cos\alpha}{\sin\alpha}. \quad (29)$$

Notice from the above expression that, if $\dot{w} \to 0$ then the airspeed will be stabilized. Analyzing V_a in (4) with $\dot{w} = 0$, it follows that the airspeed required to $\dot{w} \to 0$ is given by

$$V_a = \sqrt{\frac{-2m(qu + g\cos\theta)}{\rho S A_w(\alpha)}}. \quad (30)$$

The angle of attack of a fixed-wing drone with classical configuration satisfies that $\alpha \leq \alpha_{stall}$, where α_{stall} is the stall angle of the airplane. Notice that this angle is projected with the maximum pitch angle θ_{Max}. Therefore, the minimum airspeed can be computed through of the following expression,

$$V_{a_{min}}(\theta_{Max}) = \sqrt{\frac{-2m(qu + g\cos\theta_{Max})}{\rho S A_w(\theta_{Max})}}. \quad (31)$$

III. Landing Control Strategy

Let us consider that the airplane comes in cruise flight with constant altitude h and airspeed V_a. The control goal will be to land the fixed-wing drone at a desired landing coordinate $R_d = (x_d\,,\, z_d)$. Thus, a transition coordinate $R_T = (x_T\,,\, z_T)$ from the cruise flight to a descending maneuver needs to be computed. This transition coordinate depends on the altitude, touchdown point, a descending angle ζ_d, and the aircraft's airspeed, i.e. $R_T(h, V_a, R_d, \zeta_d)$, see Figure 1.

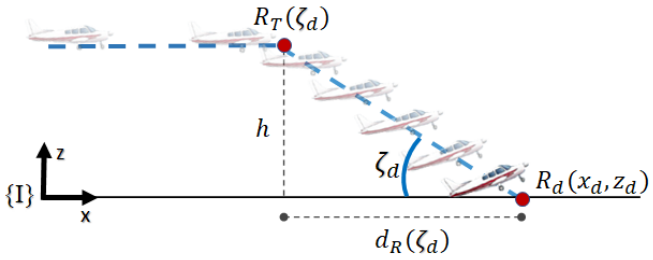

Fig. 1: Landing strategy in a specific coordinate for a fixed-wing drone with the least speed.

A. Descending angle ζ_d analysis

Let analyze the descending flight of a fixed-wing vehicle as illustrated in Figure 2. From figure, the dashed (red) line denotes the longitudinal axis where the velocity u is projected. The line (gray) with arrow describes the airspeed vector. In our analysis, a positive angle is defined as a counterclockwise angle, and a negative angle by a clockwise angle. The angle of attack α represents the angle between the longitudinal axis of the airplane and the vector V_a. The pitch angle θ describes the angle between the horizontal axis and the longitudinal axis. Finally, the flight path angle γ is represented as the angle between the airspeed vector and the horizontal axis.

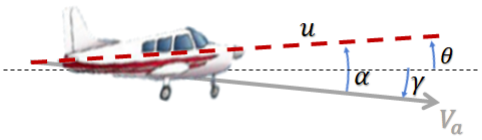

Fig. 2: Representation of the aircraft angles in the vertical plane for a descending flight.

From an aerodynamic analysis, the pitch angle is commonly described as

$$\theta = \alpha + \gamma \tag{32}$$

Notice then from Figure 2 that, γ can be used for defining the descending angle ζ_d. Observe from this figure that for $\gamma > \epsilon$ the aircraft is in ascending flight, for $\gamma < -\epsilon$ the plane is in descending flight and for $-\epsilon \leq \gamma \leq \epsilon$ the aircraft can be in cruise flight, for $\epsilon << 1$. Remember that the goal in this work is to reach a high angle of attack without lossing the controllability of the system and having a positive pitch angle, i.e. $\alpha \leq \alpha_{stall}$ & $\theta > 0$. Thus, ζ_d can be proposed as a value of γ with the constraint $-\alpha_{stall} < \gamma < \epsilon$.

Once chosen the angle ζ_d, it is possible to determine the coordinate where the airplane should begin the descending stage. This coordinate is expressed as

$$R_T(h, V_a, R_d, \zeta_d) = (x_d - d_R(\zeta_d, h),\, h) \tag{33}$$

where

$$d_R(\zeta_d, h) = \frac{h}{\tan \zeta_d} \tag{34}$$

When the aircraft reaches the coordinate R_T, the landing control strategy is applied to guide the aircraft towards R_d using the engine control input δ_t, and the airspeed reduction is performed by tracking desired pitch angles using the elevator deflection control δ_e, see Figure 1.

The desired pitch angle is defined by the following expression,

$$\theta_d(t) = \frac{\theta_{Max} - \theta_i}{d_R(\zeta_d, h)} \left(d_R(\zeta_d, h) - d\right) + \theta_i \tag{35}$$

where θ_i is the initial pitch angle taken when the airplane is in cruise flight. d represents the distance between the aircraft position $(x,\, z)$ and the coordinate R_d. This distance defines as the path parameter which is computed as follows

$$d = \sqrt{e_x^2 + e_z^2} \tag{36}$$

where $e_x = (x_d - x)$ and $e_z = (z_d - z)$.

B. Guidance control strategy

The design of a control law to guide the aircraft towards a coordinate is based on the flight path angle γ. The Lyapunov stability analysis is developed to determine an engine control input, guarantying the rendezvous at the desired point.

Propose the flight path angle as

$$\gamma_d = \tan^{-1}\left(\frac{e_z}{e_x}\right) \tag{37}$$

Therefore, the flight path angle error can be expressed as

$$e_\gamma = \gamma - \gamma_d = \theta - \alpha - \gamma_d \tag{38}$$

and then

$$\dot{e}_\gamma = \dot{\theta} - \dot{\alpha} - \dot{\gamma}_d. \tag{39}$$

Differentiating (37), it yields

$$\dot{\gamma}_d = \frac{(x_d - x)(\dot{z}_d - \dot{z}) - (z_d - z)(\dot{x}_d - \dot{x})}{(x_d - x)^2 + (z_d - z)^2}, \tag{40}$$

Propose the following positive function as

$$V_1 = \frac{1}{2} e_\gamma^2 \tag{41}$$

Differentiating the above equation and using (39) and (26), it follows that

$$\dot{V}_1 = e_\gamma\, \dot{e}_\gamma = e_\gamma \left(\dot{\theta} - \frac{u\dot{w} - w\dot{u}}{u^2 + w^2} - \dot{\gamma}_d\right) < 0. \tag{42}$$

Introducing (3) into (42), it yields

$$\begin{aligned} \dot{V}_1 = e_\gamma \Bigg[& \dot{\theta} - \frac{u\dot{w}}{u^2 + w^2} - \dot{\gamma}_d \\ & + \frac{w}{u^2 + w^2} \left(-qw - g\sin\theta + \frac{\rho V_a^2 S}{2m} A_u \right. \\ & \left. + \frac{\rho S_h C_h}{2m} \left[(k_r \delta_t)^2 - V_a^2 \right] + d_u \right) \Bigg] < 0. \end{aligned} \tag{43}$$

Proposing the following engine control input

$$\begin{aligned} \delta_t^2 = & \frac{2m}{\rho S_h C_h K_r^2} \left(qw + g\sin\theta - d_u\right) + \frac{V_a^2}{K_r^2} \left[1 - \frac{S}{S_h C_h} A_u\right] \\ & + \frac{2m(u^2 + w^2)}{\rho S_h C_h K_r^2 w} \left(-\dot{\theta} + \frac{u\dot{w}}{u^2 + w^2} + \dot{\gamma}_d - \frac{1}{2} e_\gamma \right) \end{aligned} \tag{44}$$

it follows that introducing (44) into (43), $\dot{V}_1$ becomes

$$\dot{V}_1 = -V_1 < 0. \tag{45}$$

implying that $e_\gamma \to 0$ and $\gamma \to \gamma_d$ with $w \neq 0$. Observe that in cruise flight $w \approx 0$, nevertheless, for the landing stage the altitude is varying implying that $w \neq 0$.

In real-flight scenarios, external disturbances often affect the system performance. Notice that (44) has terms associated to these external disturbances. For taking them into account, the following external disturbance observer is proposed [30],

$$\begin{aligned} \dot{\hat{u}} &= -qw - g\sin\theta + \frac{\rho V_a^2 S}{2m} A_u + \frac{\rho S_h C_h}{2m} P_u \\ &\quad + \hat{d}_u + L_{u_1}(u - \hat{u}) && (46) \\ \dot{\hat{d}}_u &= \hat{a}_u + L_{u_2}(u - \hat{u}) && (47) \\ \dot{\hat{a}}_u &= L_{u_3}\,\mathrm{sgn}\,(u - \hat{u}) && (48) \end{aligned}$$

where $\hat{u}$, $\hat{d}_u$, and $\hat{a}_u$ denote the estimations of u, d_u, and $a_u = \dot{d}_u$, respectively. L_{u_1}, L_{u_2}, and L_{u_3} are gains of positive constant value. Same procedure is applied for estimating d_w.

Therefore, using the estimated values of d_u and d_w, (44) becomes

$$\delta_t^2 = \frac{2m}{\rho S_h C_h K_r^2}\left(qw + g\sin\theta - \hat{d}_u\right) + \frac{V_a^2}{K_r^2}\left[1 - \frac{S}{S_h C_h}A_u\right] + \frac{2m(u^2+w^2)}{\rho S_h C_h K_r^2 w}\left(-\dot{\theta} + \frac{u\dot{w}}{u^2+w^2} + \dot{\gamma}_d - \frac{1}{2}e_\gamma\right) \quad (49)$$

where

$$\dot{w} \quad = \quad qu + g\cos\theta + \frac{\rho V_a^2 S}{2m}A_w + \hat{d}_w \quad (50)$$

C. Pitch dynamic stabilization

The pitch angle error e_θ can be rewritten as

$$e_\theta = \theta - \theta_d \quad (51)$$

Differentiating (51), it yields

$$\dot{e}_\theta \quad = \quad \dot{\theta} - \dot{\theta}_d \quad (52)$$

Proposing the following positive function

$$V_2 = \frac{1}{2}\eta^2 \quad (53)$$

where $\eta = e_\theta + \dot{e}_\theta$. Derivating the above equation and using (6), it follows that

$$\dot{V}_2 = \eta\left[\dot{e}_\theta + \frac{\rho V_a^2 Sc}{2J_y}\left(C_m(\alpha) + \frac{Cm_q cq}{2V_a} + Cm_{\delta e}\,\delta_e\right) + d_q - \ddot{\theta}_d\right] \quad (54)$$

From (54), the pitch dynamics can be stabilized using the following controller

$$\delta_e = \frac{1}{C_{m_{\delta_e}}}\left[-\left(C_m(\alpha) + Cm_q\frac{c}{2V_a}q\right) + \frac{2J_y}{\rho V_a^2 Sc}\left(-\dot{e}_\theta - d_q + \ddot{\theta}_d - \frac{1}{2}\eta\right)\right]. \quad (55)$$

For estimating d_q, the following external disturbance estimator is proposed

$$\dot{\hat{q}} = \frac{\rho V_a^2 Sc}{2J_y}\left[Cm_0 + Cm_\alpha\alpha + Cm_q\frac{cq}{2V_a} + Cm_{\delta e}\,\delta_e\right] + \hat{d}_q + L_{q_1}(q - \hat{q}) \quad (56)$$

$$\dot{\hat{d}}_q = \hat{a}_q + L_{q_2}(q - \hat{q}) \quad (57)$$

$$\dot{\hat{a}}_q = L_{q_3}\,\mathrm{sgn}(q - \hat{q}) \quad (58)$$

where $\hat{q}$, $\hat{d}_q$, and $\hat{a}_q$ denote the estimated values of q, d_q, and $a_q = \dot{d}_q$, respectively. L_{q_1}, L_{q_2}, and L_{q_3} are gains of positive constant value.

Using the estimated value of d_q, (55) can be expressed as

$$\delta_e = \frac{1}{C_{m_{\delta_e}}}\left[-\left(C_m(\alpha) + Cm_q\frac{c}{2V_a}q\right) + \frac{2J_y}{\rho V_a^2 Sc}\left(-\dot{e}_\theta - \hat{d}_q + \ddot{\theta}_d - \frac{1}{2}\eta\right)\right]. \quad (59)$$

Substituting (59) into (54), it yields

$$\dot{V}_2 = -V_2 < 0 \quad (60)$$

Notice that e_θ, $\dot{e}_\theta \to 0$. Then, $\theta \to \theta_d$. Observe also that when using the control laws $e_x, e_z \to 0$, therefore from (36), $d \to 0$, implying from (35) that $\theta_d \to \theta_{Max}$. And therefore, from (31) $V_a \to V_{a_{min}}(\theta_{Max})$.

IV. Numerical validation

The proposed algorithms for airspeed reduction and rendezvous in a desired coordinate are validated in numerical simulations. Table I introduces the aerodynamic and physical parameters of the fixed-wing vehicle used in simulations.

The maximum lift coefficient must be obtained to determine the stall angle. However, it is necessary to evaluate the angle of attack to obtain the maximum negative elevator's deflection $\delta_{e_{max}}$ to lead up the aircraft's nose.

Analyzing (6) for a steady cruise flight, yields

$$\delta_{e_{max}} = -\frac{C_m(\alpha)}{C_{m\delta_e}} \quad (61)$$

then

$$C_m(\alpha) = -\frac{\delta_{e_{max}}}{C_{m\delta_e}} \quad (62)$$

Therefore, the angle of attack that satisfies (62) represents the stall angle. For this simulation, the elevator's deflection is given in a range of $[-20°, 20°]$. Evaluating the previously mentioned with the aerodynamic parameters of our reference aircraft, the stall angle is given by $\alpha_{stall} = 18.8°$

In simulations, the fixed-wing drone performs a cruise flight with an altitude of 15 meters, and an airspeed of 11 m/s. The touchdown point is chosen in $R_d = (500, 0)$ in meters. The descending angle is selected as $\zeta_d = -4°$. From (34), it yields that $d_R(\zeta_d) = 214.51$ m, thus, the coordinate $R_T(\zeta_d)$ is given as $(285.49, 15)$ in meters. From the cruise flight, the pitch angle is small ($\theta_i = 1.6°$), making it our initial descending pitch angle. $\theta_{Max} \leq \alpha_{stall}$ is chosen as $\theta_{Max} = 14.8°$.

Using a wind model described in [31], the external disturbances is proposed to change in a range of $[-4, 2.6]$ m/s^2. The parameters of the disturbances estimator algorithms are selected as $L_{(\cdot)_1} = 12$, $L_{(\cdot)_2} = 80$, and $L_{(\cdot)_3} = 0.8$, with $(\cdot) : u, w, q$.

Parameters	Value	Parameters	Value
C_{L_0}	0.4029	C_{D_0}	0.0256
C_{L_α}	4.64	C_{D_α}	0.1749
C_{L_q}	7.4431	C_{D_q}	0
$C_{L_{\delta_e}}$	-0.42108	$C_{D_{\delta_e}}$	0.00528
C_{m_0}	-0.0408	C_{m_α}	-1.0454
C_{m_q}	-8.9585	$C_{m_{\delta_e}}$	-1.09407
S_h	0.0314	C_h	1
K_r	8	C_{D_p}	0.027
m	0.824	J_y	0.02453
AR	6.54	c	0.168
M	50	α_0	0.4712
S	0.185	b	1.1

TABLE I: Parameters of the aircraft used in simulations.

In Figure 3 the system performance is illustrated when the control algorithms are validated in closed loop. Notice in this figure the two flight stages (cruise and the descending flight) until the aircraft reaches the touchdown point. From this figure, the dashed (black) line represents the desired path. The dashed (red) line describes the aircraft behavior without compensante the effects of external disturbances (DST). Finally, the solid (blue) line depicts the control strategy involving the external disturbance estimator (EDE). From this figure observe that even if the aircraft reaches the touchdown point its behavior (dashed red line) presents some perturbations due to the external disturbances that are not compensated. Notice also, that when the control algorithms include the estimated values of these perturbations the performance is improved.

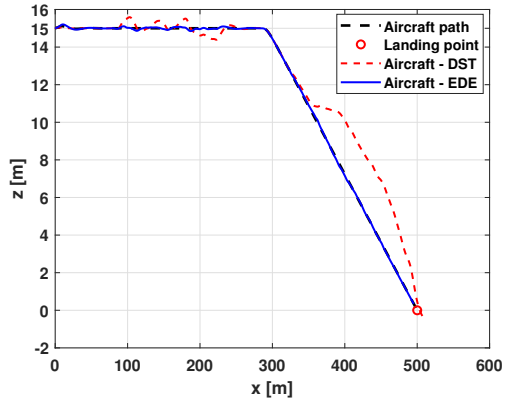

Fig. 3: Simulation results of the landing control strategy.

The pitch angle performance is presented in Figure 4. Notice here that it is increased from $2°$ to $14.8°$ following the expression (35). Analyzing the case without estimation parameters, the pitch angle is affected by the external disturbances, and some oscillations are presented leading down the aircraft's nose. Otherwise, applying the disturbance estimator algorithms, the pitch angle continues the reference tracking. Remark from Figure 5 that the aerial system reaches angles of attack close to the α_{stall}. This is due when the pitch angle is increased for the airspeed reduction. Notice also from this figure, that the angle of attack remains small in cruise flight.

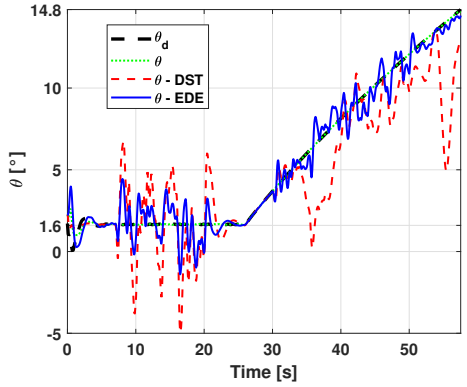

Fig. 4: Performance of the pitch angle tracking.

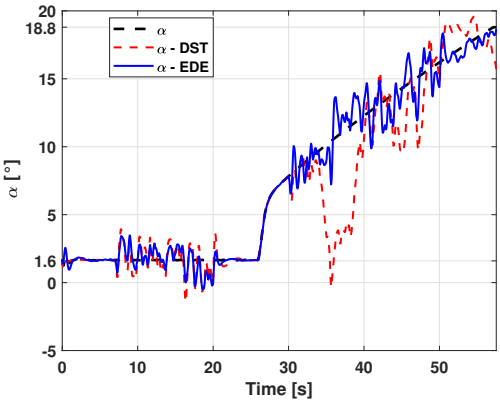

Fig. 5: Behavior of the angle of attack during the control strategy.

In our analysis, we demonstrated the relationship between the angle of attack and the airspeed. Therefore, if the aircraft navigates a high speed its angle of attack is small, and at low speed a high angle of attack can be obtained for airspeed reduction, see Figure 6. From this figure, notice that when the control algorithm is used without parameters estimation, the airspeed increases when the aircraft is perturbed (see dashed red line). Therefore, when the estimated parameters are considered in the control laws the airspeed reduction is done gradually without showing strong perturbations. Observe also that the minimum value obtained for V_a is of 5.9m/s.

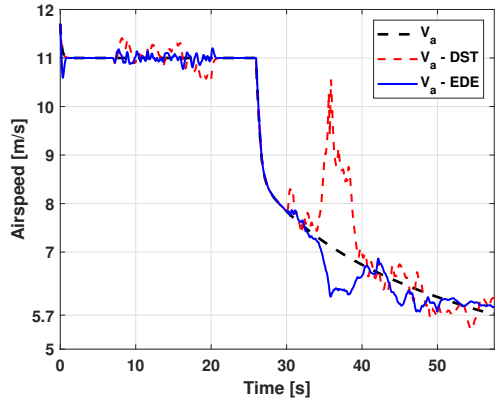

Fig. 6: Airspeed reduction along of the landing strategy.

In Figure 7 the behavior of the flight path angle is introduced. For a cruise flight, notice that γ tends to zero. In the descending stage, the flight path angle goes to the descending angle ζ_d. Notice that in the case without parameters estimation, the aircraft becomes unstable before of the touchdown point.

Figure 8 represents the performance of the engine control input, δ_t. Observe that the motor power tends to reduce at the descending stage. In addition, we can notice the difference in the variations produced by the perturbations, considering (or not) the estimated parameters. Similarly, Figure 9 illustrates the elevator performance, δ_e. A negative deflection produces leading up the aircraft's nose. Notice that the negative deflection increases until its limit of $-20°$ to

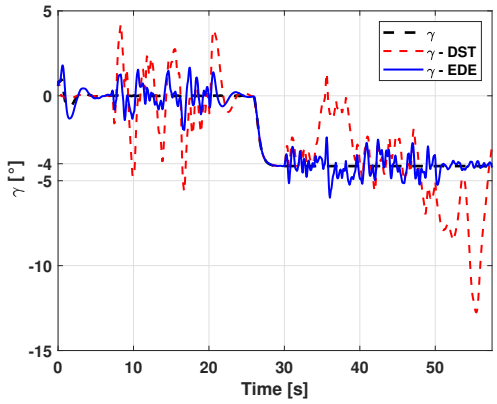

Fig. 7: Performance of the flight path angle to guide the aircraft towards landing point.

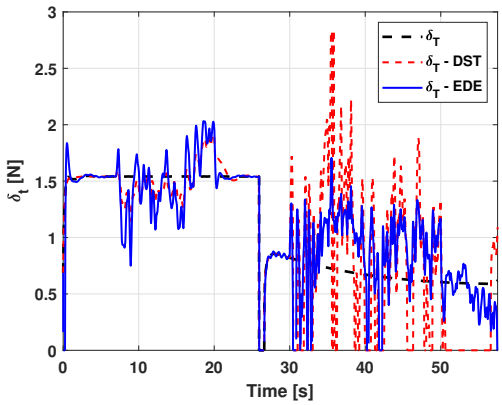

Fig. 8: Behavior of the engine control input.

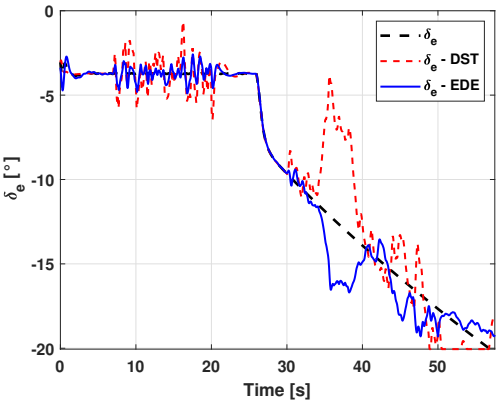

Fig. 9: Elevator deflection for the airspeed reduction.

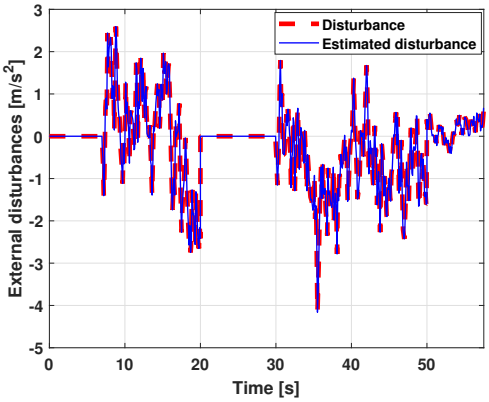

Fig. 10: Performance of the observer algorithm for external disturbances.

reduce the airspeed while the aircraft is guided to the desired point. The elevator reaches its limit to obtain the maximum angle of attack before the stall angle.

Finally, Figure 10 shows the performance when the external disturbances are estimated. These estimated values were included in the control law for compensating the disturbance effects involving the aircraft performance. Notice the well estimation of these parameters.

V. Conclusions

A control strategy for landing a fixed-wing drone on a predefined coordinate was proposed in this work. The control strategy was conceived for airspeed reduction during the landing stage. This airspeed reduction was done when the pitch angle was increased gradually until reaching a maximum value close to stall angle that defines the stability of the aerial system. The control laws were obtained using the Lyapunov theory and an observer was proposed for estimating external aerodynamics parameters. Simulations demonstrated the well performance of the control strategy in closed loop system.

Future work

In future work, the whole dynamics of the aircraft will be considered for developing a nonlinear and robust control strategy. An experimental platform is being developed and practical validation of the landing control strategy is also considered as future work.

Acknowledgment

This paper was supported by the RPV project - UTC foundation and the Mexican National Council of Science and Technology - CONACyT.

References

[1] Š. Čerba, J. Lüley, B. Vrban, F. Osuský, & V. Nečas. “Unmanned radiation-monitoring system”. IEEE Transactions on Nuclear Science, 67(4), 636-643, 2020.

[2] X. C. Ding, A. R. Rahmani, & M. Egerstedt. “Multi-UAV convoy protection: An optimal approach to path planning and coordination”. IEEE transactions on Robotics, 26(2), 256-268, 2010.

[3] I. Mahmud, & Y. Z. Cho. “Detection avoidance and priority-aware target tracking for UAV group reconnaissance operations”. Journal of Intelligent & Robotic Systems, 92(2), 381-392, 2018.

[4] T. Oliveira, & P. Encarnação. “Ground target tracking control system for unmanned aerial vehicles”. Journal of Intelligent & Robotic Systems, 69, 373-387, 2013.

[5] T. Ahilan, V. A. Adityan, & S. Kailash, S. “Efficient Utilization of Unmanned Aerial Vehicle (UAV) for Fishing through Surveillance for Fishermen”. International Journal of Aerospace and Mechanical Engineering, 9(8), 1468-1471, 2015.

[6] P. Iscold, G. A. Pereira, & L. A. Torres (2010). “Development of a hand-launched small UAV for ground reconnaissance”. IEEE Transactions on Aerospace and Electronic Systems, 46(1), 335-348, 2010.

[7] L. Merino, F. Caballero, J. R. Martínez-de Dios, J. Ferruz & A. Ollero. “A cooperative perception system for multiple UAVs: Application to automatic detection of forest fires”. Journal of Field Robotics, 23(3-4), 165-184, 2006.

[8] S. Bhandari, A. Bettadapura, O. Dadian, N. Patel, J. Dayton, & M. Gan, “Search and rescue using unmanned aerial vehicles”. In AIAA Infotech@ Aerospace, (p. 1458), January 5-9, 2015. Kissimmee, Florida.

[9] E. Ackerman, & M. Koziol. “The blood is here: Zipline’s medical delivery drones are changing the game in Rwanda”. IEEE Spectrum, 56(5), 24-31, 2019.

[10] P. C. Garcia, R. Lozano, and A. E. Dzul. “Modeling and Control of Mini-Flying Machines”. Springer-Verlag, London.

[11] M. Varga, J. C. Zufferey, Heitz, G. H. M. Zufferey, & D. Floreano. “Evaluation of control strategies for fixed-wing drones following slow-moving ground agents”. Robotics and Autonomous Systems, 72, 285-294, (2015).

[12] T. Elijah, R. S. Jamisola, Z. Tjiparuro, & M. Namoshe. “A review on control and maneuvering of cooperative fixed-wing drones”. International Journal of Dynamics and Control, 9(3), 1332-1349, (2021).

[13] D. Zhang, & X. Wang. “Autonomous Landing Control of Fixed-wing UAVs: from Theory to Field Experiment”. J Intell Robot Syst 88, 619–634 (2017).

[14] M. Ruchanurucks, P. Rakprayoon, & S. Kongkaew. “Automatic landing assist system using IMU+ PnP for robust positioning of fixed-wing UAVs”. Journal of Intelligent & Robotic Systems, 90(1), 189-199, 2018.

[15] O. A. Yakimenko, I. I. Kaminer, W. J. Lentz, & P. A. Ghyzel. “Unmanned aircraft navigation for shipboard landing using infrared vision”. IEEE Transactions on Aerospace and Electronic Systems, 38(4), 1181-1200, 2002.

[16] B. Barber, T. McLain, & B. Edwards. “Vision-based landing of fixed-wing miniature air vehicles”. Journal of Aerospace Computing, Information, and Communication, 6(3), 207-226, 2009.

[17] H. J. Kim, M. Kim, H. Lim, C.Park, S. Park, D. Lee, & Y. Kim. “Fully autonomous vision-based net-recovery landing system for a fixed-wing UAV”. IEEE/ASME Transactions On Mechatronics, 18(4), 1320-1333, 2013.

[18] “Landing A Drone Aircraft With No Runway: SkyHook Recovery System”. [Online] https://www.youtube.com/watch?v=J4uJ4yShEDA&t=2s - Consulted on (11/12/2022).

[19] M. Moghadam, N. K. Ure, & G. Inalhan. “Autonomous execution of aircraft supermaneuvers with switching nonlinear backstepping control”. AIAA Guidance, Navigation, and Control Conference, p.1594, January 8–12, 2018. Kissimmee, Florida.

[20] A. K. Tripathi, V. V. Patel, & R. Padhi. “Autonomous landing of fixed wing unmanned aerial vehicle with reactive collision avoidance”. IFAC-PapersOnLine, 51(1), 474-479, February 18-22, 2018. Hyderabad, INDIA.

[21] Rotondo, D., Cristofaro, A., Gryte, K., & Johansen, T. A. “LPV model reference control for fixed-wing UAVs”. IFAC-PapersOnLine, 50(1), 11559-11564, July, 9-14, 2017. Toulouse, France.

[22] M. J. Tahk, S. Han, B. Y. Lee & J. Ahn. “Trajectory optimization and control algorithm of longitudinal perch landing assisted by thruster”. In 2016 European Control Conference (ECC) (pp. 2247-2252), IEEE. June 29 - July 01 , 2016. Aalborg, Denmark.

[23] S. Shao, J. Liu, J. Shan, W. Zeng, & S. Liu. “Optimization and Trajectory Tracking of Deep Stall Landing for a Variable Forward-swept Wing UAV”. In 2022 5th International Symposium on Autonomous Systems (ISAS) (pp. 1-6), IEEE. April 8-10, 2022. Hangzhou, China.

[24] S. H. Mathisen, T. I. Fossen, & T. A. Johansen. “Non-linear model predictive control for guidance of a fixed-wing UAV in precision deep stall landing”. International Conference on Unmanned Aircraft Systems (ICUAS) pp. 356-365, IEEE, June 9-12, 2015. Denver, CO, USA.

[25] S. H. Mathisen, K. Gryte, T. Johansen, & T. I. Fossen. “Non-linear model predictive control for longitudinal and lateral guidance of a small fixed-wing UAV in precision deep stall landing”. In Aiaa infotech@ aerospace, p. 0512, January 4-8, 2016. San Diego, California, USA.

[26] S. Mathisen, K. Gryte, S. Gros, & T. A. Johansen. “Precision deep-stall landing of fixed-wing UAVs using nonlinear model predictive control”. Journal of Intelligent & Robotic Systems, 101(1), 1-15, 2021.

[27] R. W. Beard, & T. W. McLain. “Small unmanned aircraft: Theory and practice”. Princeton university press, 2012.

[28] K. Gryte. “High angle of attack landing of an unmanned aerial vehicle”. Master’s thesis, Norwegian University of Science and Technology (NTNU- Trondheim), 2015.

[29] R.F. Stengel “Flight Dynamics”. Princeton, NJ: Princeton Univ. Press, 2004.

[30] J. Yang, C. Liu, M. Coombes, Y. Yan & W.H. Chen. “Optimal path following for small fixed-wing UAVs under wind disturbances”. IEEE Transactions on Control Systems Technology, 29(3), 996-1008, 2020.

[31] A. Chapman, A., & M. Mesbahi. “Uav flocking with wind gusts: Adaptive topology and model reduction”. American Control Conference; pp. 1045-1050. IEEE. June 29 - July 01, 2011. San Francisco, CA, USA.